



Article

Can Forel–Ule Index Act as a Proxy of Water Quality in Temperate Waters? Application of Plume Mapping in Liverpool Bay, UK

Lenka Fronkova ^{1,*} , Naomi Greenwood ^{1,2} , Roi Martinez ¹, Jennifer A. Graham ^{1,2} , Richard Harrod ¹, Carolyn A. Graves ¹, Michelle J. Devlin ^{1,2,3} and Caroline Petus ³

- ¹ Centre of Environment, Fisheries and Aquaculture Science, Pakefield Rd, Lowestoft NR33 0HT, UK; naomi.greenwood@cefas.co.uk (N.G.); roi.martinez@cefas.co.uk (R.M.); jennifer.graham@cefas.co.uk (J.A.G.); richard.harrod@cefas.co.uk (R.H.); carolyn.graves@cefas.co.uk (C.A.G.); michelle.devlin@cefas.co.uk (M.J.D.)
- ² Collaborative Centre for Sustainable Use of the Seas, University of East Anglia, Norwich NR4 7TJ, UK
- ³ TropWater, James Cook University, Townsville, QLD 4811, Australia; caroline.petus@jcu.edu.au
- * Correspondence: lenka.fronkova@cefas.co.uk; Tel.: +44-(0)-1502524431

Abstract: The use of ocean colour classification algorithms, linked to water quality gradients, can be a useful tool for mapping river plumes in both tropical and temperate systems. This approach has been applied in operational water quality programs in the Great Barrier Reef to map river plumes and assess trends in marine water composition and ecosystem health during flood periods. In this study, we used the Forel–Ule colour classification algorithm for Sentinel-3 OLCI imagery in an automated process to map monthly, annual and long-term plume movement in the temperate coastal system of Liverpool Bay (UK). We compared monthly river plume extent to the river flow and in situ water quality data between 2017–2020. The results showed a strong positive correlation (Spearman’s rho = 0.68) between the river plume extent and the river flow and a strong link between the FUI defined waterbodies and nutrients, SPM, turbidity and salinity, hence the potential of the Forel–Ule index to act as a proxy for water quality in the temperate Liverpool Bay water. The paper discusses how the Forel–Ule index could be used in operational water quality programs to better understand river plumes and the land-based inputs to the coastal zones in UK waters, drawing parallels with methods that have been developed in the GBR and Citclops project. Overall, this paper provides the first insight into the systematic long-term river plume mapping in UK coastal waters using a fast, cost-effective, and reproducible workflow. The study created a novel water assessment typology based on the common physical, chemical and biological ocean colour properties captured in the Forel–Ule index, which could replace the more traditional eutrophication assessment regions centred around strict geographic and political boundaries. Additionally, the Forel–Ule assessment typology is particularly important since it identifies areas of the greatest impact from the land-based loads into the marine environment, and thus potential risks to vulnerable ecosystems.

Keywords: earth observation; ocean colour; Forel–Ule; Liverpool Bay; Great Barrier Reef; Sentinel-3; river plume; water quality



Citation: Fronkova, L.; Greenwood, N.; Martinez, R.; Graham, J.A.; Harrod, R.; Graves, C.A.; Devlin, M.J.; Petus, C. Can Forel–Ule Index Act as a Proxy of Water Quality in Temperate Waters? Application of Plume Mapping in Liverpool Bay, UK. *Remote Sens.* **2022**, *14*, 2375. <https://doi.org/10.3390/rs14102375>

Academic Editors: Teodosio Lacava, Hanwen Yu, Mi Wang, Jianlai Chen and Ying Zhu

Received: 15 February 2022

Accepted: 19 April 2022

Published: 14 May 2022

Publisher’s Note: MDPI stays neutral with regard to jurisdictional claims in published maps and institutional affiliations.



Copyright: © 2022 by the authors. Licensee MDPI, Basel, Switzerland. This article is an open access article distributed under the terms and conditions of the Creative Commons Attribution (CC BY) license (<https://creativecommons.org/licenses/by/4.0/>).

1. Introduction

Traditionally, water quality assessments have been conducted within a set of geographical or political boundaries that do not necessarily reflect ecological processes. These geographical constraints can prevent assessments from being made across a river to coast continuum [1,2]. In the United Kingdom (UK), the coastal and marine environmental status is determined within geographically defined regions (typologies) under several European Directives, such as the Water Framework Directive (WFD), OSPAR Common Procedure and UK Marine Strategy [3,4]. However, a new approach defining the water quality assessments recently emerged, which can better reflect the physical, chemical and

biological processes present in the water. This approach involved mapping river plumes using satellite derived particulate matter (SPM) and in situ salinity [2]. Although this method can provide assessments across ecologically homogeneous areas, defining river plumes seasonally and on a relatively high resolution in the coastal areas is needed to assess the water quality conditions across estuarine and intertidal habitats.

Using the colour of the ocean retrieved by optical satellite imageries to determine the water condition and map river plumes has been an emerging method that can be applied worldwide using the ocean colour multispectral satellite products on a low to medium spatial resolution [5–9]. This has been particularly relevant in the tropical waters of the Great Barrier Reef (GBR), where the use of ocean colour satellite products to map river flood plumes is a key part of the GBR marine monitoring program, and is reported on an annual basis for wet season monitoring [10–12]. Historically, the monitoring of the river plumes across the GBR has been conducted using Moderate Resolution Imaging Spectroradiometer (MODIS) ocean colour satellite data and based on a supervised classification into three optical waterbodies, namely Primary, Secondary and Tertiary wet season water types. The Primary water type is associated with low salinity from river discharge and plume waters but can also reflect re-suspended sediment from wind and tides. The Secondary water type is often associated with relatively less turbid water and is typically found in the open coastal and outer flood plume waters of the GBR. Tertiary waters are found in the mid-shelf and offshore waters of the GBR and have a low risk of detrimental ecological effects. The frequency of the wet season optical water types were used in a risk assessment to define habitats likely exposed to land-based pollutants and integrated in an operational framework to assess trends in marine water composition and ecosystem health during flood periods [13]. Recently, the GBR plume mapping has been tested on the Sentinel-3 OLCI satellite data, linking the original plume waterbody classes to the Forel–Ule Index (FUI) [11]. This method is now used operationally in the GBR Marine Monitoring Program (MMP) [14].

The Forel–Ule (FU) colour scale was developed at the end of the 18th century by Forel [15] and Ule [16] to visually identify optical water types using a scale consisting of 21 colour classes, ranging from indigo blue to cola brown. The Forel–Ule Index (FUI) was then derived from the FU scale in the chromaticity diagram using X, Y, Z tristimulus values in the 1930s [17], which correspond to the red (X), green (Y) and blue (Z) in the visible range of the light spectrum [18], and this created the basis of the latest FUI algorithms [6,7,19,20]. As a part of the European EC-FP7 Citclops project (Citizens’ Observatory for Coast and Ocean Optical, URL: <http://www.citclops.eu/home>, accessed on 1 April 2020), a consistent and objective classification algorithm of natural water into the FUI was developed, using remote sensing reflectance (Rrs) or water leaving radiance of the ocean colour [6,19,21]. The algorithm was incorporated into the European Space Agency (ESA) open-source SNAP software (hereafter, FUI satellite toolbox). The FUI satellite toolbox currently takes five satellite products as input data (SeaWiFs, CZCS [6], MERIS [6,22], MODIS [6,8,10] or OLCI Sentinel-3 A and B [6,11]), which allows data with varying spatial and temporal resolution to be processed. The advantage of multiple satellite instruments is their potential combination to reduce missing values and extend the timeseries.

In addition, the main aim of the Citclops project was the development of affordable citizen science tools that can measure different water properties. A smartphone application called EyeOnWater Colour was created which provides a fast assessment of surface water colour on the FUI scale from the user’s phone camera. In situ measurements from the application contribute to standardised historical measurements of the FUI [21,23,24], and have been used to validate the FUI classes derived from the FUI satellite toolbox. A successful uptake of the FUI satellite toolbox lies in its ease of processing, potential for detailed mapping of nearshore and marine waterbodies and estimating biological, physical and chemical characteristics of the water [21]. The FUI has been linked to the water quality parameters, such as the amount of nutrients present in the water, SPM, turbidity

or salinity [5,25]. As such, the FUI can be used to map the river plume extent and act as a proxy of water quality.

Ensuring long-term monitoring of coastal water quality is important in both tropical reefs and temperate ecosystems, since sensitive marine habitats can be detrimentally affected by poor water conditions. Although corals have a certain degree of resistance to the warming sea temperatures, it has been demonstrated that corals which regularly experience poor water conditions, such as elevated dissolved inorganic nitrogen (DIN), are less resistant to thermal stress. As a result, the modelling shows that the corals' upper thermal bleaching limits can be reduced significantly with a decrease in DIN [26]. Other studies also show that the coral reef management through improved water quality will increase the overall survival potential of corals to climate change [27]. Similarly, the abundance of seagrass meadows was linked with the amount of contaminants present in the water. The increased SPM with turbidity can result in decreased light availability for the seagrass photosynthesis, hence its abundance [28,29]. An elevated amount of nutrients can stimulate the seagrass growth; however, over-enrichment would ultimately lead to an increased amount of plankton and macroalgae, which in turn could reduce light attenuation and cause a reduction in the seagrass communities [30]. As such, declining water quality has significant impacts on the GBR coastal ecosystems, where land sourced pollution transported in river flood plumes has been a key driver in inshore coral and seagrass habitat loss [8,24].

The application of the FUI to map long-term changes in the extent of the river plume and assess the relevance of this methodology for operational water quality monitoring programs has never been applied in the UK waters. In this paper, we explore the application of the FUI to map monthly and annual river plumes in Liverpool Bay (UK) between 2017–2020 using Sentinel-3 A and B OLCI satellite data. The changes in the river plume extent are compared to the river flow from a combination of fifteen rivers discharging into Liverpool Bay. Furthermore, the GBR water type classification is applied in Liverpool Bay and assessed against another water type classification developed in the European Citeclops project for temperate regions. The comparison provides insight on the application of the FUI categories to define optical water types - in different geographic and climatic regions. The paper also links the FUI classes with in-situ water samples and draws conclusions on its suitability to act as a proxy for water quality monitoring programs in the UK. It can be an important tool in defining water quality assessment typologies that are based on the optical properties, and hence supplement the current approaches using geographically and politically delimited typologies.

2. Materials and Methods

2.1. Study Area

Liverpool Bay (Figure 1) is a shallow (<50 m) sub section of the eastern Irish Sea, receiving substantial freshwater inputs from several rivers [31]. In this case study, we focus on assessing the freshwater inputs of fifteen rivers and their tributaries in the Liverpool Bay catchment area. The name of each river, its principal location and the contributing gauges are depicted in Figure 1. Riverine plumes are the major transport mechanism for nutrients, sediments and other land-based pollutants into the bay. Liverpool Bay is a complex hydrodynamic system, where the vertical and horizontal stratification and mixing of the freshwater plume is determined by tides. The tides influence the geographic location and dispersion of the river plume sediments, nutrients and biological composition of the water [31]. As such, mapping the river plume extent, its cycles and variations can provide useful insight on the water constituents and its quality.

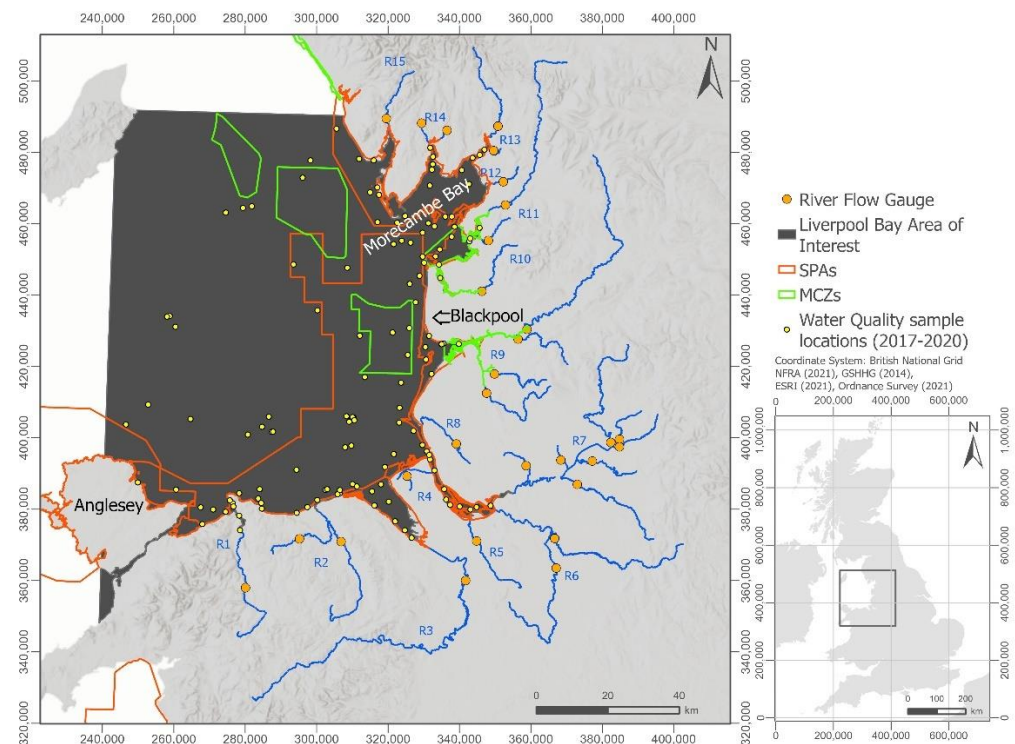


Figure 1. Location of Liverpool Bay and the river data used for the analysis. The orange circles show the positions of 29 gauges used to measure the river flow of the following rivers: R1—Conwy, R2—Clwyd and Elwy, R3—Dee, R4—Arrow Brook, R5—Gowy, R6—Dane and Weaver, R7—Bollin, Glaze, Irk, Irwell, Medlock, Mersey and Sankey, R8—Alt, R9—Darween, Douglas, Ribble, Yarrow, R10—Wyre, R11—Lune and Conder, R12—Keer, R13—Bela and Kent, R14—Crake and Leven, R15—Duddon. Green and orange polygons denote Special Protection Areas (SPAs) and Marine Conservation Zones (MCZs).

The northwest region of Liverpool Bay is highly populated, with more than 7 million people in 2011, which has risen by approximately 5% since the 2001 census, collected by the Office for National Statistics (ONS). The greatest population density is located in the Greater Manchester area and city of Liverpool [32]. In 2018, North Wales had a total estimated population of approximately 700,000, with Flintshire being the most densely populated authority [33]. Increased human activities and changes in the land management might cause pressure on the ecosystems and their exposure to pollution. In 2019, the dominant farm types in the northwest were grazing livestock farms, accounting for 59% of the total farmed area, followed by dairy, which covered 19% of the farmed area [34]. Overall, Liverpool Bay receives high riverine nutrient inputs resulting in elevated nutrient concentrations in coastal waters, although algal biomass is not sufficient for it to be classified as eutrophic [2,4,35]. The SPM and riverine input of terrestrial Coloured Dissolved Organic Matter (CDOM) influence the underwater light amount in the area [3,36]. In addition, the sediment dynamics are a primary concern in Liverpool Bay, since the sand dune system, which actively erodes and expands, acts as natural protection to the coast. The sand dunes are a tourist attraction and their changes are important for the marine shipping of the Liverpool international port [31]. Liverpool Bay contains eight designated OSPAR Special Protection Areas (SPAs) and five Marine Conservation Zones (MCZs) (Figure 1). These areas provide habitat and protection for various species such as red-throated diver, common scoter and little gull [37], and the important recreation and commercial fishing species European sea bass (*Dicentrarchus labrax*) and thornback ray (*Raja clavata*) [38]. Furthermore, Liverpool Bay includes seagrass, saltmarsh and seaweed ecosystems, which act as blue carbon storage and also provide nursing and spawning grounds [39]. For all these listed

reasons, Liverpool Bay has become a focal point of the scientific research on the impact of the freshwater loads onto the bay's hydrodynamics and water quality.

2.2. Water Quality Monitoring

Surface data (<5 m depth) for 1 January 2017–31 December 2020 were obtained for the study area for the inorganic nutrients, namely nitrite, nitrite + nitrate, silicate, phosphate and ammonium, turbidity, SPM, salinity and Chl-a. Data were collated from national monitoring programmes operated by several UK government agencies in the region. Estuarine and coastal water quality data collected under the Water Framework Directive were obtained from the Environment Agency (Open WIMS data) and Natural Resources Wales. Coastal and offshore data collected under the Marine Strategy Framework Directive were obtained from Cefas and Agri-Food and Biosciences Institute (Afbi) (Supplementary Material Table S1). Sample collection and processing was carried out by each of the agencies and detailed methods are presented in [2] and references therein. Briefly, surface samples were typically collected from a depth between 2 m to 4 m and subsampled for nutrients, SPM, turbidity, salinity and Chl-a. Turbidity was determined using turbidity meters and converted to SPM using discrete samples collected and analysed for SPM. Salinity was determined either using a calibrated conductivity meter or from discrete samples analysed using a calibrated salinometer. Nutrients were estimated using colorimetric methods, and Chl-a was measured on acetone extracts of filtered samples analysed using a calibrated fluorometer [2]. The monthly aggregated FUI values were extracted at the locations of the in situ water quality samples (Figure 1) using Python 3 arcpy library, and the relationships between the water parameters and FUI were explored statistically by calculating the Spearman's rho and showing the relationship graphically.

2.3. River Flow Data

River gauge data were extracted, for each of the major freshwater sources into Liverpool Bay, from the National River Flow Archive (NRFA, Supplementary Material Table S1). Gauged daily flow rates were extracted for each location over the period of interest, from 1 January 2017–30 September 2020. Sources were chosen based on those closest to the river mouth, and available during the period of interest, with the location of all contributing gauge sites for each of the fifteen rivers shown in Figure 1. Where a single source was not available for significant lengths of time (e.g., for Mersey at Westy, NRFA station 69037), gauges were combined from each of the available rivers and tributaries upstream. Where data were missing for occasional days during the timeseries, flow rates were filled using the median value for that site. For comparison with the river plume area monthly satellite composites, daily flow rates were then summed over each month, to provide the total volume of river discharge into Liverpool Bay.

2.4. FUI Satellite Mapping of Water Type

Waterbodies of Liverpool bay were mapped applying the FUI on the Sentinel-3 OLCI A and B satellite data, according to both the Citclops project [21] and GBR [11] waterbody types. The waterbody types are defined using different -categories of FUI and reflect -reflect the physical, chemical and biological properties of the water. In the Citclops project, five waterbody types are defined, ranging from indigo blue to greenish blue waters (FUI classes 1–5) that correspond to waters with high light penetration. These waters often have low nutrient levels and low production of biomass. The colour is dominated by microscopic algae (phytoplankton). The greenish blue to bluish green (FUI classes 6–9) corresponds to waters with a colour still dominated by algae, but also increased dissolved organic matter and some suspended sediment may be present. The FUI 1–9 is classified as the Open Sea. The greenish waters (FUI classes 10–13 for Coastal waters) correspond to Coastal waters which usually display increased nutrient and phytoplankton levels, but also contain suspended sediment and dissolved organic material. The greenish brown to brownish green waters (FUI classes 14–17 for Near-Shore water) reflect waters with high

nutrient and phytoplankton concentrations, but also increased suspended sediment and dissolved organic matter. They are typical for Near-Shore areas and tidal flats. Finally, the brownish green to cola brown waters (FUI classes 18–21 for Estuary waters) relate to waters with an extremely high concentration of humic acids, and are typical for rivers and Estuaries [21] (Summary in Table 1). The method of measuring the FUI classes in the field is using a Secchi disk and 21 coloured glasses is depicted in Figure 2. In the GBR plume typology, $FUI \geq 10$ values are grouped into a unique waterbody referred as Primary water type, while $FUI 6-9$, $FUI 4-5$ and $FUI \leq 3$ are referred to as Secondary, Tertiary and Marine water types, respectively [11] (summary in Table 1). According to these waterbody properties, it is possible to infer water quality condition based on the links made between FUI and in situ nutrients [5,12,21,25].

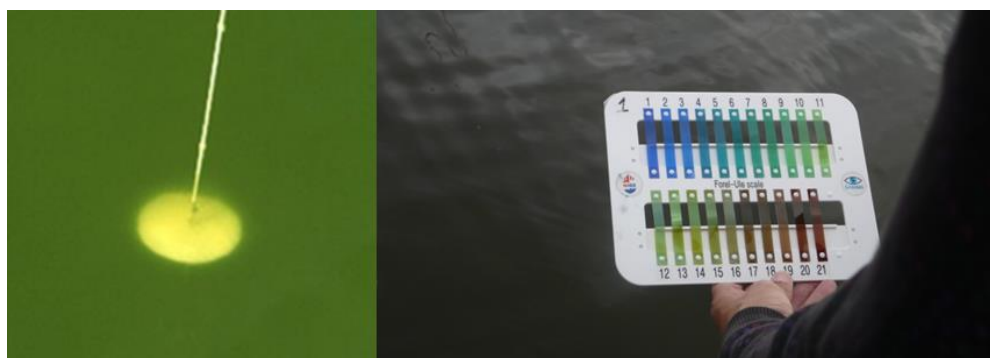


Figure 2. Measurement of water colour using a Secchi disk and Forel-Ule colour scale (source Reproduced with permission from Ceccami et al., PLOS ONE, 2020, <https://doi.org/10.1371/journal.pone.0230084>).

Table 1. Water type classification and their description.

Source	Water Type (Classes)	FUI	Description
Petus et al., 2019 [11]	Primary	≥ 10	High concentration of phytoplankton, nutrients, sediments and decreased light attenuation
	Secondary	6–9	Dominated by algae, but increased dissolved organic material and some sediment
	Tertiary	4–5	High light penetration
	Marine	1–3	High light penetration
Citclops (http://www.citclops.eu/home , accessed on 1 April 2020)	Estuaries	18–21	Extremely high concentration of humic acids typical for rivers and Estuaries
	Near-shore	14–17	High nutrient and phytoplankton, increased sediment and dissolved organic material typical for Coastal waters
	Coastal	10–13	Increased nutrient and phytoplankton, some minerals and dissolved organic material
	Open Sea	1–9	Dominated by microscopic algae, some sediment might be present but typically the Open Sea

2.5. FUI Batch Processing

We used a seven steps method, that is graphically shown in Figure 3, to compute daily FUI outputs using Sentinel-3 data, clean coastal outliers and aggregate and interpolate any missing data into monthly and climatological river plume composites in Liverpool Bay between 2017–2020. Firstly, the Sentinel-3 A and B water Level-2 product was downloaded from EUMETSAT (Sentinel-3 data sources are present in Supplementary Material Table S1). The Level-2 water leaving reflectance was produced by EUMETSAT after applying either a Baseline Atmospheric Correction, which removes the pixel glint and white caps and is mainly used for the open waters, or an alternative neural network atmospheric correction that is more suitable for the turbid waters [40].

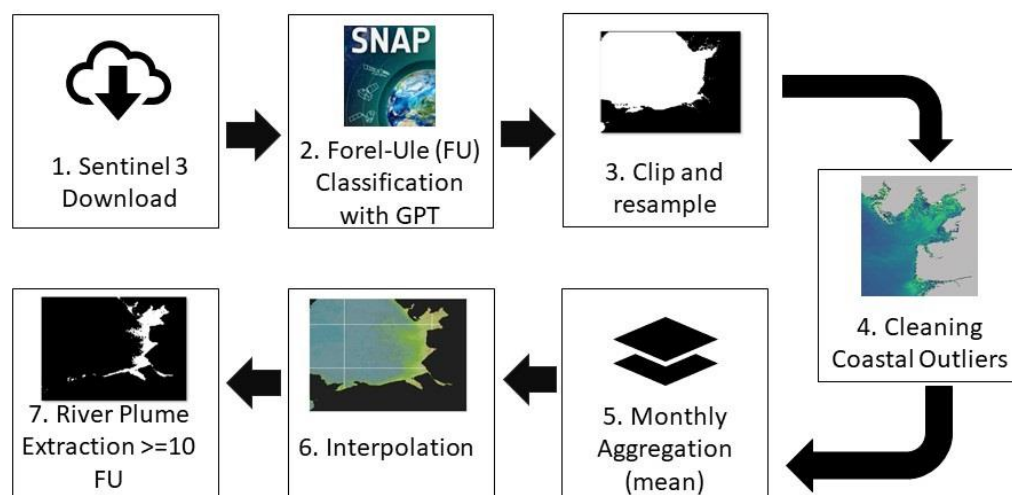


Figure 3. A schematic diagram of the methodology used to extract river plume in Liverpool Bay.

In the next step, FUI was calculated using the SNAP Graph Processing Tool (GPT), which enables a batch processing of timeseries data. The processing graph applied the “FU Classification” algorithm developed in the Citclops project [6,7,18,21]. The FU Classification algorithm derives the true colour of natural waters based on the calculation of tristimulus values, which are the three parameters (X, Y, Z) that determine the colour stimulus of the human eye [17,41]. The CIE 1931 Colour Matching Function (CMF) determines the weights of the tristimulus values in the red (X), green (Y) and Z (blue) wavelengths (λ). The tristimulus values are then converted by a series of functions presented in [7,18,19] into the water hue angle (α) which corresponds to the 21 FUI colour classes. The calculation of FUI in the step 2 of Figure 2 was followed by resampling and clipping the data to a common grid to create a 3D array (a raster stack) for the temporal analysis. Values $FUI \leq 5$ were removed from the coastal areas, which are suspected to originate from the changes in water levels, where a pixel’s reflectance can be affected by the bottom reflectance during low tides (step 4).

Due to frequent cloud cover in the UK, the daily FUI was aggregated to monthly composites using the mean FUI value (step 5). The mean aggregation of FUI was used in other studies such as [42], and it is preferred over median as it uses all the data and smooths the extreme values. Missing data were interpolated using inverse distance weighting with the search radius of ~ 1 km (step 6). The last step involved extracting pixels $\geq FUI 10$, which were classified as the river plume. The threshold of FUI 10 to delineate the inner boundary of a plume was used both in the Citclops project and GBR Marine Monitoring Program. It corresponds to the brownish colour on the FU scale, which is linked to higher SPM loads, lower salinity and increased nutrients (Table 1) [21]

Frequency composites were computed per year and the whole timeseries to map spatially how many times a pixel was flagged as a river plume. The FUI monthly products were then classified according to the Citclops and GBR water type classification (Section 2.4). However, due to a low frequency of FUI in the class 1–5, this class was merged with the class 6–9 for the Citclops project categories as illustrated in Table 1. The analysis was conducted in an automated Python 3 script, using open source (steps 1, 4, 5, 6, 7) and arcpy libraries (step 3). The scripts are available in a public GitHub repository at: https://github.com/CefasRepRes/forel_ule (DOI: 10.5281/zenodo.6074090, accessed on 14 February 2022).

3. Results

3.1. Plume Extent

The spatial distribution of the plume is consistent across the whole timeseries between 2017–2020 in Liverpool Bay (Figure 4). Pixels marked as river plume more than 75% of the

time (freq. > 0.75) follow a contour of shallow waters (<10 m) from the coast. In addition, the plume frequency maps highlight a transitional area that changes annually off the coast of Blackpool (Figure 1), creating a bulge that extends towards the open sea. This is caused by the presence of the Shell Flat sandbank, an area of shallow depth (<15 m) that extends 10 nm offshore from Blackpool. This area is classified as a plume between 50 to 75% of the sampling period (freq. = 0.5–0.75), with the largest area in 2019. Pixels marked as plume 25% or less (freq. \leq 0.25) are transient plume features which could be linked to the interannual fluctuations in the river flow, or artefacts created during the data processing resulting from missing data values due to clouds. The majority of the transient plume pixels are not deeper than 30 m (Figure 4). Morecambe Bay, which is an outlet of multiple rivers depicted in Figure 1 (Crake and Leven, Bela and Kent, Keer, Lone and Conder, Wyre), shows the presence of the largest freshwater plume extent off the coast of Liverpool Bay, which is constant across the timeseries (Figure 4). This could be caused by the tidal and current processes in the sheltered Morecambe Bay, that can hold the run-off longer, as opposed to more open coastal areas, such as the coast of North Wales.

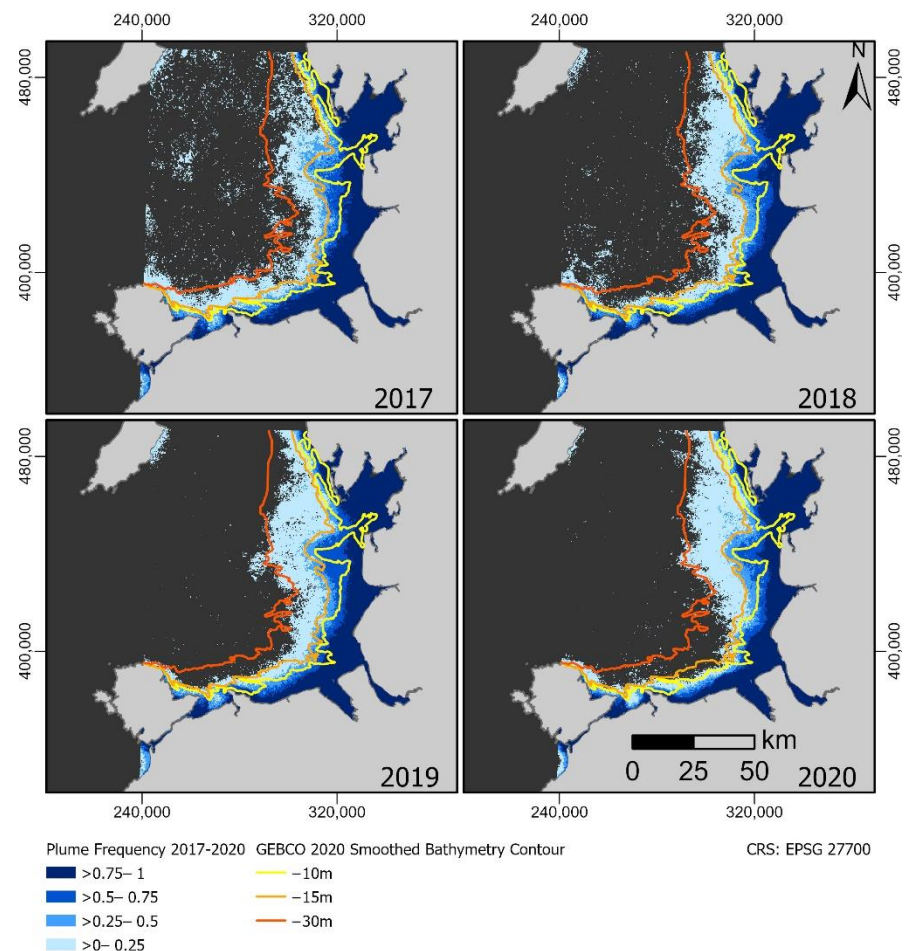


Figure 4. Yearly plume frequency in the Liverpool Bay. The plume frequency 1 denotes the pixel was marked as plume in all the months within the year. The mapped river plume corresponds to the Coastal, Near-Shore and Estuaries waterbodies (FUI \geq 10) [21] and Primary plume (FUI \geq 10) wet season class from [11]. The source of bathymetry is: GEBCO Compilation Group (2020) GEBCO 2020 Grid doi:10.5285/a29c5465-b138-234d-e053-6c86abc040b9, accessed on 1 February 2022.

Annual and seasonal variations in river plume extent between 2017 and 2020 are illustrated in Figures 5 and 6 after classifying the FUI into the waterbody types from the Citclops project and GBR. In this classification, the Primary waterbodies, relating to a higher concentration of nutrients, SPM and CDOM [11], representing the freshwater plume,

correspond with the Coastal, Near-Shore and Estuaries waterbodies from the European Citclops project [21]. However, the European classification provides more detailed waterbody classes within the Primary plume area, whereas the GBR FUI methodology has only one class within the plume extent and three classes in the open waters. Overall, both methods provide the same definition of the plume extent of $FUI \geq 10$, which shows that the definition of the river plume based on this threshold could be applied in various geographic locations. Applying two geographically distinct FUI waterbody clusters used across Europe and GBR highlight a need to define the local clustering waterbody types for Liverpool Bay, which contains a more turbid water system. The importance of the locally defined classification lies in their use for risk mapping, where the risk is calculated as magnitude (waterbody type) \times likelihood (frequency) [13], hence having an effect on the potential monitoring program.

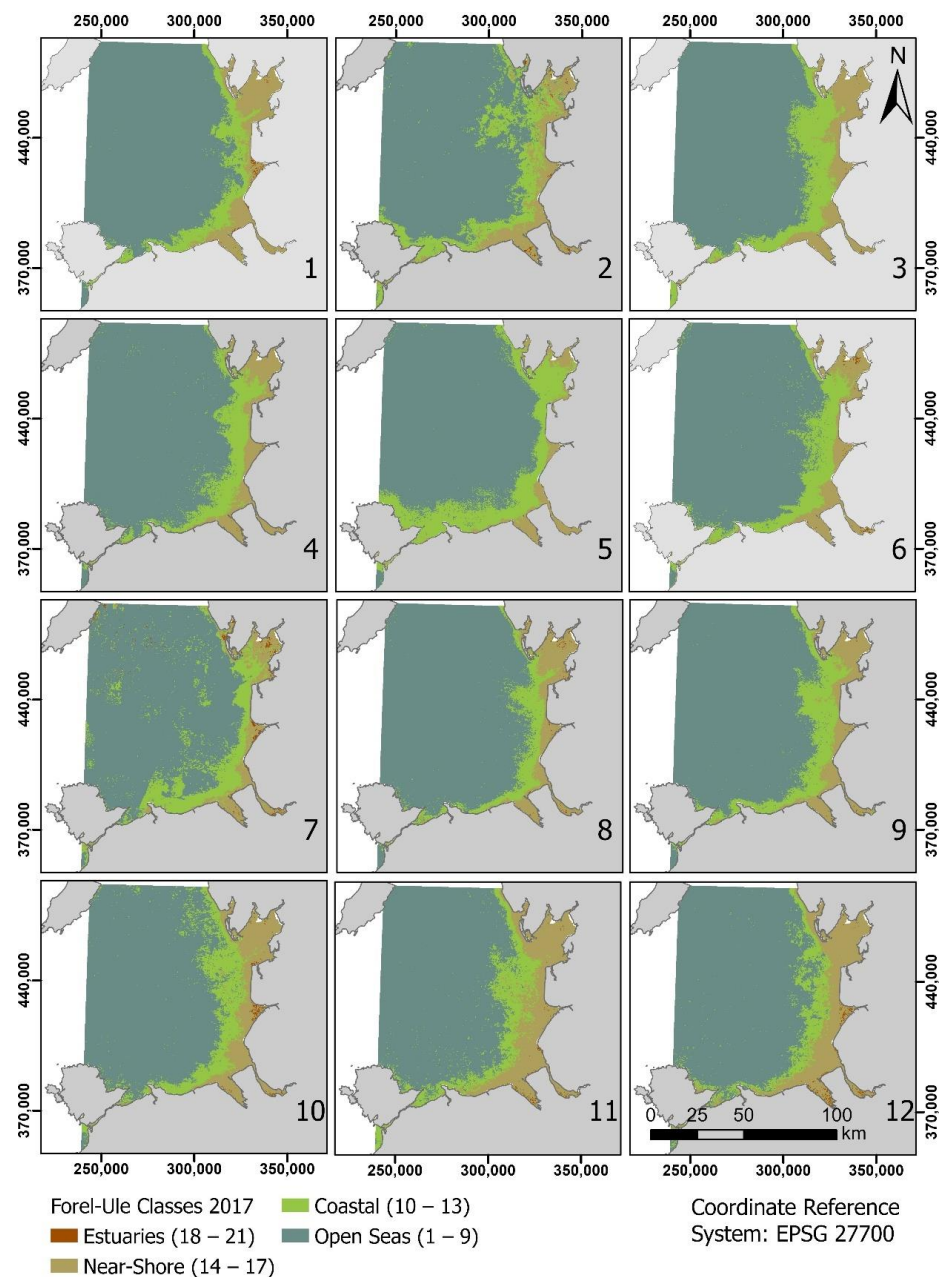


Figure 5. Spatial changes observed in the river plume extent (FUI between 10–21) in 2019 suggest the presence of three seasons: 1. wet season (months: 12, 1, 2, 3); 2. dry season (months: 5, 6, 7, 8) and 3. mixed season (months: 4, 9, 10, 11).

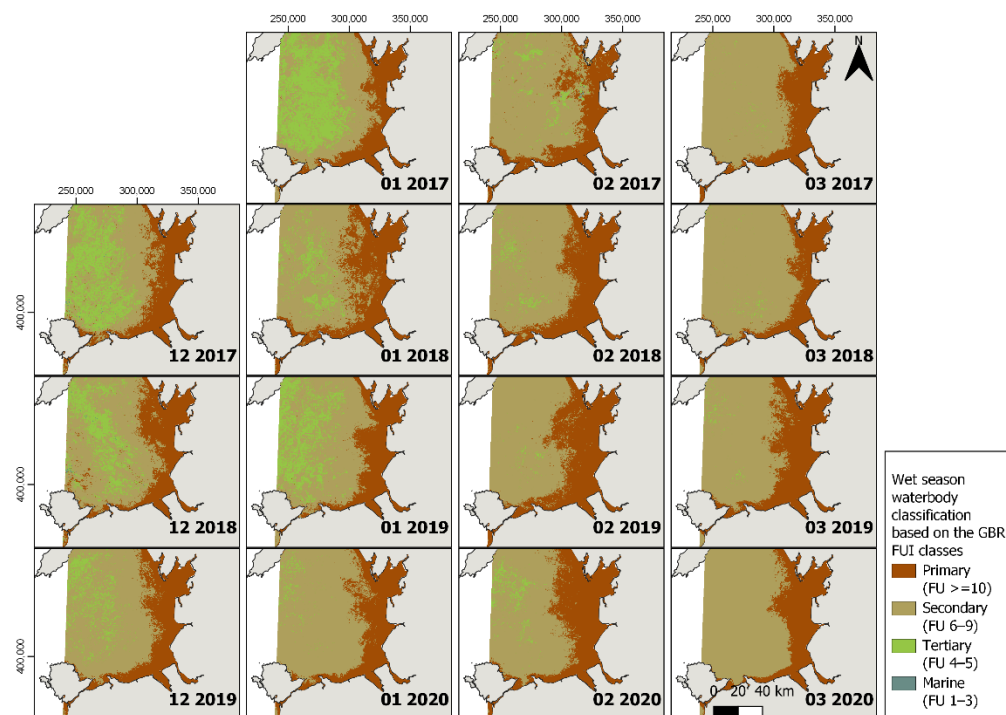


Figure 6. Classification of Liverpool Bay wet season (December, January, February, March) according to the four GBR waterbody classes based on FUJ values. The river plume areas across the wet season between 2017–2020 do not change significantly across the months.

Annually, the largest average plume extent of 2336 km² is measured in 2017 (Table 2). This might be related to a wetter than normal summer season, which is shown by the larger plume area measured in May, June, July and August 2017 (Figure 7). Years 2018, 2019 and 2020 exhibit a more pronounced seasonal pattern than 2017. In this period, the plume extent fluctuates seasonally, displaying three distinct trends: (1) a wet season (December, January, February, March), (2) a dry season (May, June, July, August) and (3) a mixed season (April, September, October, November). In the wet season, the average plume area is greater by approximately 40%, compared to the dry season in 2018, 2019 and 2020 (Table 2).

Table 2. Descriptive statistics for the annual and seasonal river plume area (km²) between 2017–2020 in Liverpool Bay, showing the average, maximum (Max), minimum (Min), standard deviation (STD) and the average per season per year.

Year	Average	Max	Min	STD	Average Dry Season	Average Wet Season	Average Mixed Season
2017	2336	2915	1807	306	2130	2442	2435
2018	2231	3290	1407	586	1707	2799	2187
2019	2273	3640	1493	682	1625	3006	2187
2020	2091	3596	1333	628	1581	2695	1998

The standard deviation within the year is similar for 2018, 2019 and 2020, but lower in 2017. In 2017 the plume area does not show the same reduction over May–July and remains constant around 2000–2500 km². The seasonal fluctuations of the plume area in 2018, 2019 and 2020 can be observed spatially in Figure 5 and Supplementary Material Figures S1–S3. In these figures, the FUJ was classified into the Citclops-defined waterbodies described in Table 1. The extent of the plume drops after February, following a downward trend until it reaches its minimum in June and July in the middle of the dry season.

The seasonal pattern of the total river plume area closely follows the river flow, which is typically highest around February and decreases through May and June for 2018, 2019 and

2020 (Figure 8). Despite a decrease in river flow in April–May 2017, the river plume area remains larger (Figures 7 and 8), suggesting other environmental or processing factors may explain plume variability in this year. Similarly, the kernel density distribution curve of 2017 differs from the remaining years, overlapping only the middle or interquartile range values of 2018, 2019 and 2020 (Supplementary Material Figure S4). Despite the differences between 2017 and the other years, the relationship between the river flow and the plume area is demonstrated by a strong positive correlation $\rho = 0.704$ ($p < 0.01$) calculated from 45 observations between 2017–2020 (Figure 9B). Since the river flow and plume data did not satisfy the requirement of a normal distribution needed to calculate Pearson’s R correlation (Supplementary Material Figure S5), Spearman’s rho was calculated instead. In terms of interannual seasonality, Figure 9A shows that a plume area threshold value between 2000–2500 km² separates the dry and wet seasons in 2018, 2019 and 2020. Beyond 2500 km², 85% of the datasets belong to the wet season. Similarly, around 75% of the dry season data occur below the 2000 km² plume area and 0.5×10^9 m³ month⁻¹ of the river flow. However, the difference between the mixed and wet season river flow data is less due to a higher flow variability in the mixed months, hence an overlap between the mixed and wet season values (Figure 9A).

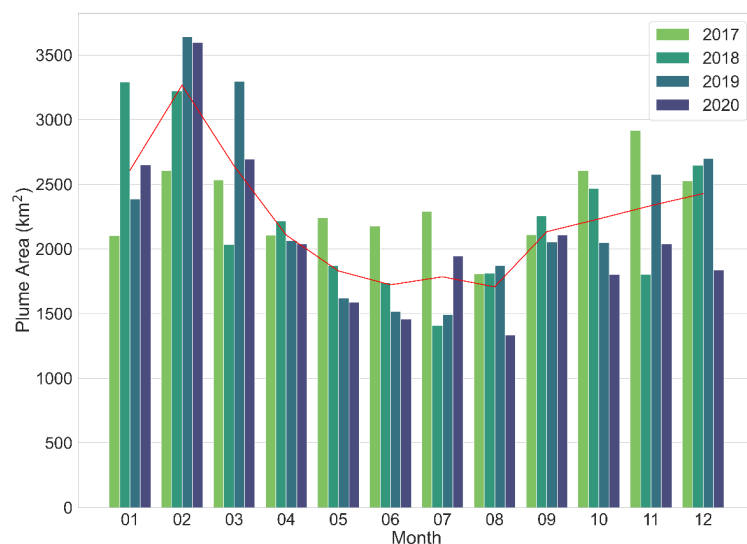


Figure 7. Total plume extent per month between 2017–2020 and the monthly average per year (red line) show the variability across the months in the timeseries.

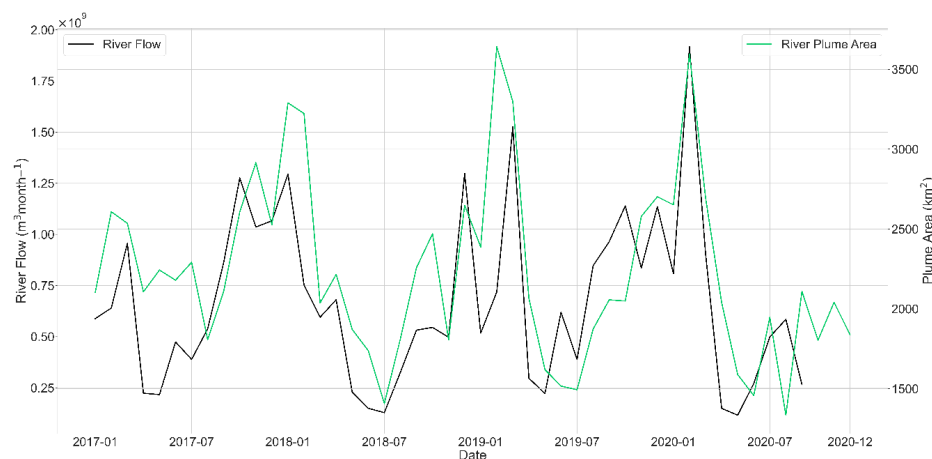


Figure 8. A timeseries of the river flow in the Liverpool Bay versus the river plume area between January 2017 and September 2020. October, November and December 2020 river flow measurements were unavailable at the time of the manuscript preparation.

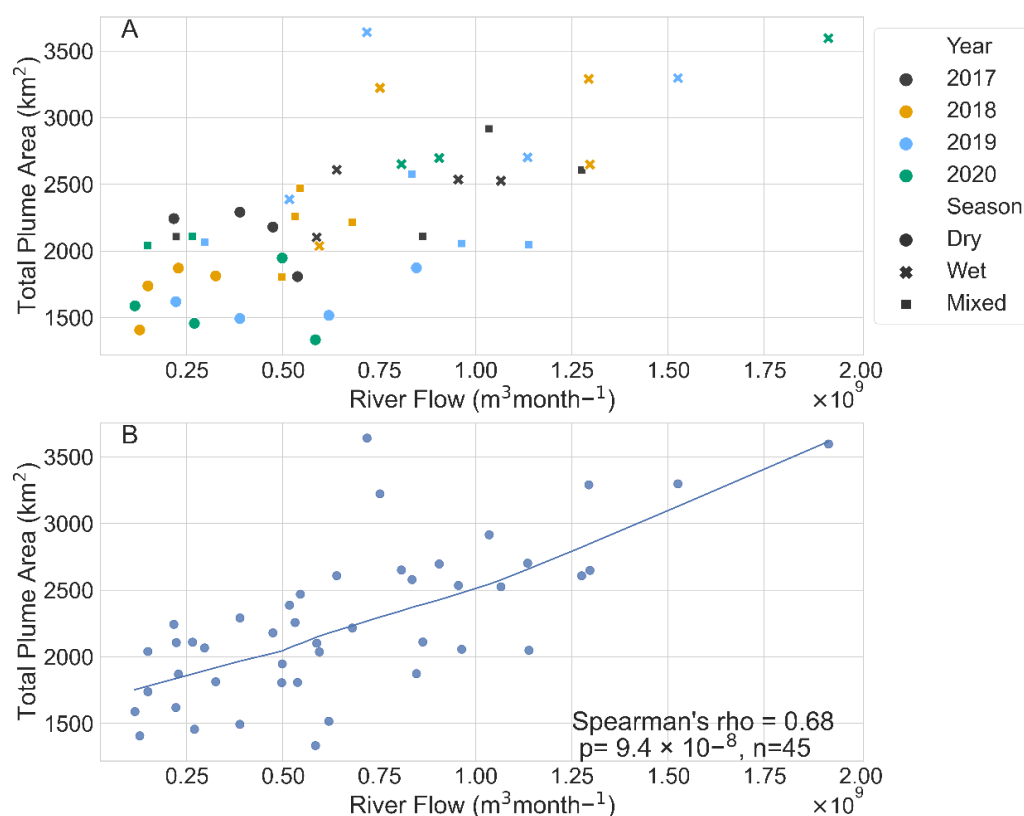


Figure 9. Variability in the river flow and the plume across years and season (A). Spearman's correlation coefficient (ρ /rho) (B) calculated between the river flow and the plume using all the available data between 2017–2020 ($n = 45$). The blue line shows the local regression fit.

3.2. FUI and Water Quality Indicators

The in situ SPM, turbidity and Chl-a all show a skewed or non-normal distribution (Supplementary Material Figure S6). The correlation between FUI values and nutrients shows a strong positive relationship for ammonium ($\rho = 0.66$), nitrite ($\rho = 0.62$), nitrite and nitrate ($\rho = 0.67$), phosphate ($\rho = 0.67$) and silicate ($\rho = 0.67$), which all exhibit a p value $< 2.2 \times 10^{-16}$, suggesting the relationship is statistically significant (Figure 10). The strongest relationship was found between the FUI and both turbidity ($\rho = 0.77$) and SPM ($\rho = 0.74$), while salinity has a strong negative correlation ($\rho = 0.61$) with FUI. The negative relationship between salinity and the FUI was expected, since the areas closer to the coasts are in general less saline and contain more nutrients from the riverine inputs, hence higher FUI values. Chl-a has a moderate correlation ($\rho = 0.4$) with the FUI. These results suggest the FUI classification can be linked to a gradient of nutrient, SPM and salinity concentrations, providing information on water types outside of in situ sampling.

The relationship between nutrients, SPM, salinity, turbidity and Chl-a is also demonstrated after grouping FUI values into the four Citclops water types (Table 1). Overall, there is an increase in nutrients in Estuaries which gradually lowers with the distance from the coast. As such, the lowest value of the nutrients is present in the Open Sea waters as depicted in Figure 11. Nutrients in the Estuaries show a distinguishable boxplot/distribution of values, which contrasts with the Near-Shore waters that display substantial variability with many extreme values. Chl-a has low variation in values across the four water classes, with the highest peaks in the Near-Shore. SPM and turbidity have slightly higher values around the Estuaries, decreasing towards the Open Seas. Salinity has a reversed trend compared to the rest of the tested variables, since it is the highest in the Open Seas and decreases sharply towards the Estuaries. Overall, the Open Seas and Coastal classes defined by the FUI are similar to each other across the tested variables, although the Coastal class shows a higher number of extreme values. In addition, the Near-Shore waters have the

highest variation, which overlaps with some of the distribution of the Estuaries, but only in the third quartile (Q3) of the boxplot values. Estuaries have distinctive high nutrient values compared to Coastal and Open Seas.

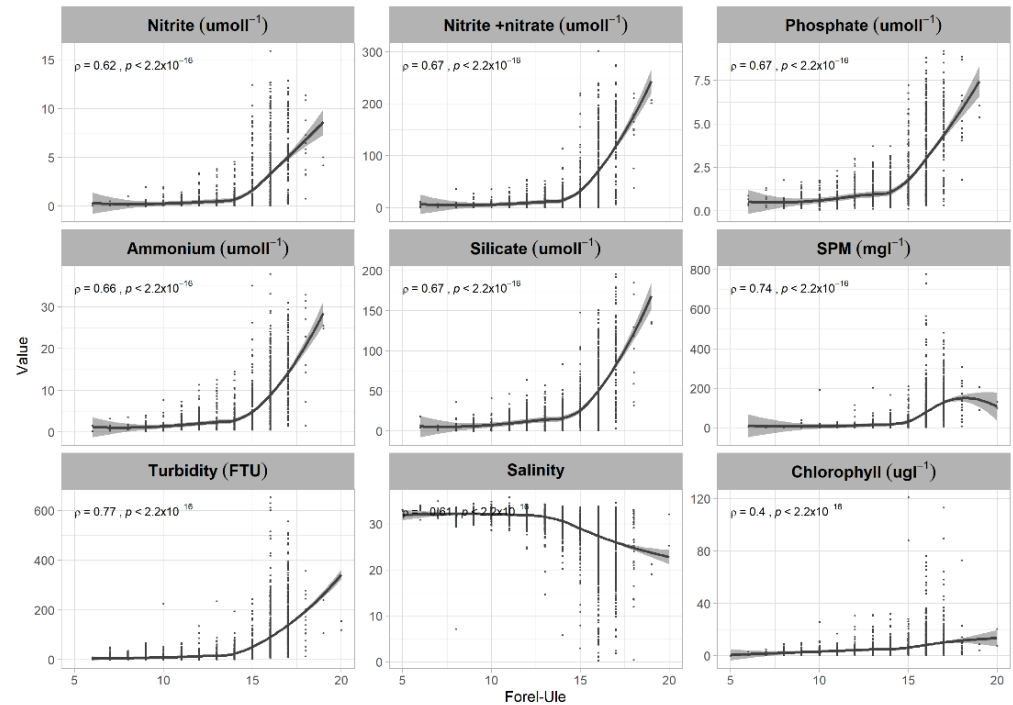


Figure 10. Spearman’s correlation (ρ /rho) with the significance value (p) between the FUI values (1–21 scale) and the water nutrients, Chl-a, SPM and turbidity. The middle line shows the local regression fit.

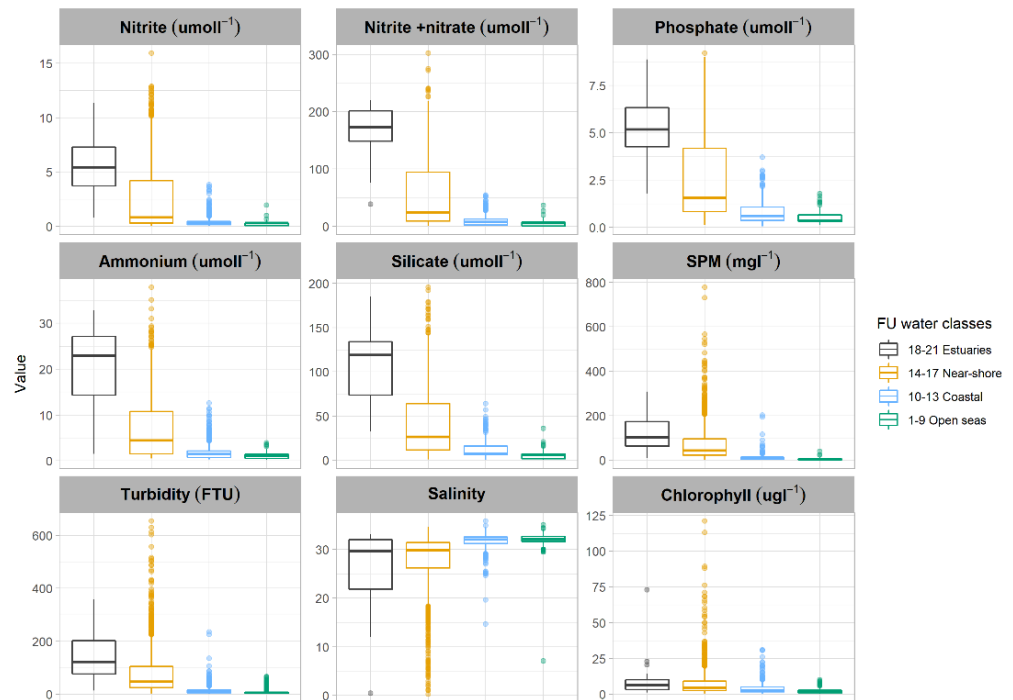


Figure 11. Whisker boxplots showing quartile distribution of water nutrients, chlorophyll-a, salinity and SPM in four Forel-Ule Citeclops water classes: 1. Estuaries, 2. Near-Shore, 3. Coastal and 4. Open Seas.

3.3. FUI Plume Typology for Water Quality Assessments

The Liverpool Bay plume extent derived from the FUI data can be used to refine the typologies used for the eutrophication assessments, especially because the results from this study show the FUI river plumes are linked with the water quality indicators, more specifically SPM, turbidity, nutrients and salinity (Section 3.2). The Forel–Ule Plume between 2017–2020 presented in this study, and the Liverpool Bay Plume, which is the SPM derived river plume typology developed in [2], align well between the rivers Clwyd and Elwy (R2) to Duddon (R15) (Figures 1 and 12). The Liverpool Bay Plume has a pronounced “nose” feature extending in the middle of the bay that is smaller in the Forel–Ule Plume; however, they follow the same general pattern (Figure 12). The Forel–Ule Plume increases the coastal resolution and provides additional information further west around the Conwy (R1) Estuary and the Anglesey Island in North Wales, as well as in the coastal areas of the northern part of the Liverpool Bay. The Forel–Ule Plume encompasses the existing WFD Coastal and Transitional eutrophication assessment areas and extends into the coastal OSPAR plume area, thereby defining the full extent of the riverine plume across these two assessment frameworks. The majority of the Forel–Ule Plume falls within the Intermittently Stratified and Permanently Mixed Ecohydrodynamic areas and the Liverpool Bay from the COMP2 typology (Figure 12).

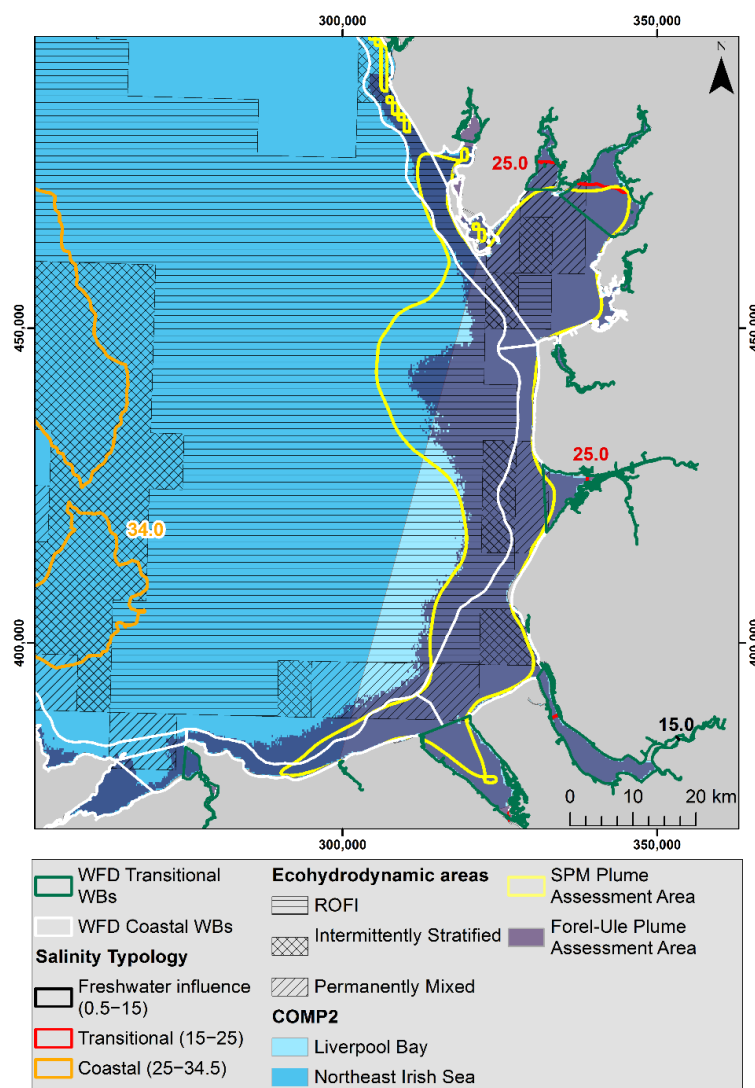


Figure 12. Traditional water quality assessment typologies in Liverpool Bay, compared to the newly defined Forel–Ule Plume.

4. Discussion

4.1. Water Quality Assessments Based on the Plume Mapping

This study provides the first low to medium resolution river plume mapping on a monthly, annual and climatological basis between 2017–2020 in the Liverpool Bay. The importance of the automated workflow developed in this study is mapping river plumes in a fast, cost-effective and reproducible way by estimating riverine influence on Coastal and Open Sea water using a combination of high spatial and temporal resolution Sentinel-3 ocean colour product and the open-source SNAP FUI algorithm. Applying Sentinel-3 OLCI satellite data to map plumes in the Liverpool Bay provides detailed plume information, thanks to its 300 m resolution. Compared to the previous studies, it uses higher resolution than MODIS or SeaWiFS (1.0 km and 1.1 km resolution, respectively) [6,10], and better radiometric resolution than MERIS [6].

Sentinel-3 OLCI is a relatively new satellite mission, increasingly applied to map river plumes [11,13]. The FUI index for the Sentinel-3 products has been used worldwide, including in the GBR, to assess water quality changes in marine waters and has already been recognised as a continuation of older ocean colour products, such as MODIS, in the long-term water monitoring programs in the GBR [11]. As such, using the FUI is not only an objective method of mapping optical water types, including river plumes, applicable worldwide, but it also provides an option to compare regions without the full knowledge of the inherent properties of the water. Thanks to the high spatial, temporal and radiometric resolution of Sentinel-3 OLCI it was possible to map river plumes with a higher definition and accuracy than in a previous assessment [2] on monthly, yearly and climatological scales from the coastal to offshore waters. The results of this study can be used to improve current water quality programs in the Liverpool Bay by refining existing assessment areas.

Formal eutrophication assessments, such as those under WFD and OSPAR, have traditionally used geographically defined assessment areas [2], whereas using the FUI to define assessment areas based on river plumes would encompass the full spatial extent of terrestrial impact in the marine environment. This would provide a more holistic approach, since it reflects the nutrient, sediment and other anthropogenic loads from the land to sea, and the specific local hydrological circulations that determine the level of mixing and the extent of the river plume. In comparison to the more recent assessment areas based on SPM or salinity [2], the SPM and FUI derived plumes are expected to be similar, as shown in Figure 12. This is due to a high correlation between the FUI and SPM, since SPM is one of the CPAs directly influencing the optical property of water which the FUI is based on. However, the FUI plume maps the river plume also off the coast of Northern Wales, which is not present in the SPM-based plume. In contrast, the FUI plume is smaller around the area of the Shell Flat sandbank off the coast of Blackpool. The discrepancies could be due to the FUI also being influenced by CDOM, Chl-a and other CPAs, which do not appear in the satellite-derived SPM plume from [2]. As such, the use of the FUI to map river plumes is based on more input data that are directly linked with the plumes (CDOM, Chl-a or SPM), hence is more representative of the freshwater loads to the sea.

The FUI is an important tool to operationally assess water quality and flood plume influence in the tropical waters of the GBR. Changing extent of river flood plumes have been linked with an increase in extreme weather [12], which is expected to intensify under IPCC climate change scenarios [43]. More extreme and frequent weather events can lead to increased inputs of sediments, nutrients and other pollutants into the coastal seas through river floods. The large-scale flooding has been linked to a decline in the health of inshore seagrass communities and coral reefs in the GBR [12]. In addition, numerous studies around the world [44–46] have shown that a change in land management, together with climate change, can result in coastal darkening. Coastal darkening is a phenomenon mainly present off the coast, where increased concentrations of light absorbing and scattering material, such as SPM or CDOM, are suggested to result in a lower amount of available light, hence darkening. This phenomenon was observed in centennial water samples in the North Sea, and was linked to delays in phytoplankton blooms [46]. As such, an increase in

the number of extreme weather systems and changes in land use in the catchments draining into the Liverpool Bay could detrimentally impact the coastal and intertidal ecosystems due to increased run-off into the sea. Cost-effective, repetitive and large-scale monitoring of water type through mapping river plumes presented in this paper could facilitate the definition of measures to ensure water quality.

4.2. Future Work and Application

The method applied in this paper to map river plumes provides new information on the spatial and temporal variations in the plume extents and provides an estimation of water quality through specific waterbodies, but also highlights where additional work is needed to progress the systematic detection of river plume waters in UK waters. Firstly, this paper suggests that despite the 21 FUI colour classes being applicable worldwide, it is important to assess the FUI clustering into waterbody types locally, hence reflecting regionally specific optical water characteristics. Both GBR and Citclops waterbody classification in the Liverpool Bay identify the river plume has an $FUI \geq 10$. In GBR, this represents the Primary river plume [11], whereas this category represents Estuaries, Near-Shore and Coastal class in the Citclops project [21]. The Citclops classes, however, provide more detailed river plume information and its water quality condition around the coast, which was found to be more suitable for mapping plumes in the Liverpool Bay. Conversely, the GBR classification offers more information on the FUI below 10, as opposed to Citclops in offshore waters, which is more adapted to the clearest tropical waters of the GBR. In the Liverpool Bay case study, two original open-water classes had to be merged into one due to lack of FUI between 1–5 in the bay. We propose keeping the Citclops classes for the river plume ($FUI \geq 10$), meaning Estuaries (FUI 18–21), Near-Shore (FUI 14–17) and Coastal (FUI 10–13), but adding more definition in the original Open Sea class (FUI 1–9) from the GBR FUI classification (Table 1), which would offer more spatial information away from the coast. As such, a detailed cluster analysis of the classes across the timeseries will be carried out in the future for the Liverpool Bay.

Another improvement of the current method lies in using ocean colour gap-free products. Since Sentinel-3 OLCI is a passive sensor, it does not penetrate through the cloud cover and the accuracy of the FUI depends on the number of cloudless images. The presence of clouds creates a significant uncertainty in the temperate regions affected by frequent passes of oceanic frontal systems, such as UK waters. Similarly, the concentration of clouds in a specific area of the daily Sentinel-3 image resulted in an uneven distribution of the available data. Consequently, it was not possible to interpolate data both spatially and temporarily to daily gap-free images. Using a combination of different satellite and modelled data in a single gap-free ocean colour product could solve this problem in the future. However, ocean colour gap-free products used, for example, to map the monthly global FUI using the European Space Agency Ocean Colour Climate Change Initiative (CCI) have a resolution of ~4 km at the Equator [42], which can be unsuitable in the coastal and intertidal areas.

This study shows that the FUI could be used as a proxy for qualitative assessment of water in Liverpool Bay, which is in agreement with the studies conducted in other geographic locations, such as the North Sea, Celtic Sea [5,25] or GBR [9,11,12]. More specifically, SPM or turbidity showed a strong positive correlation with the FUI in the above areas and Liverpool Bay, whilst Chl-a suggests a weak positive correlation [5]. Nutrients analysed in this study differ from the previous work, which focused primarily on assessing dissolved inorganic nitrogen (DIN) or dissolved inorganic phosphate (DIP) and the FUI [11,47]. Nutrient concentrations are highest in the Estuaries, Near-Shore or Coastal waters (or GBR Primary waterbody), and decrease with distance from the coast, in agreement with the description of the water quality in the waterbodies applied from Table 1 and [12]. To further analyse the relationship between water quality constituents and the FUI in Liverpool Bay, CDOM, which is one of the primary colour-producing agents and was examined in the previous work [5,25], will be included in the future assessment. Similarly,

this study did not analyse temperature and water depth, which are physical properties that can indirectly affect optical properties, as well as having been shown to be highly correlated with the FUI [5,25]. Although explaining the degree of the river plume variance by the tested variables is beyond the scope of this work and we looked at the relationship of the variables with the FUI individually, a regression model that would identify their relative importance to the river plume area is proposed for future work together with the river plume modelling. In addition, as depicted in Figure 1, the in situ water samples are primarily located in the Estuaries and Near-Shore waters, hence the water data are biased towards the Coastal areas. To improve the validation dataset and obtain a better understanding of the relationship between the FUI and water quality constituents, more in situ samples from the open waters need to be analysed.

5. Conclusions

For the first time, this study showed the potential of using a combination of Sentinel-3 and the FUI as an objective tool to map waterbodies in Liverpool Bay, and infer the biological, physical and chemical properties of the water, hence its quality. We suggest using the Cიტclops classes to categorise the FUI into specific waterbodies in Liverpool Bay, however, refining the offshore/open-water class ($FUI \geq 9$) to reflect more water categories. This case study therefore highlights the need for regionally derived FUI plume waterbody classes which reflect local variability in the optically active compounds. The presence of clouds hinders the use of the high temporal resolution Sentinel-3 data at temperate latitudes. Merging multiple satellite and modelled data could provide better coverage, but potentially reduce spatial resolution. An increased temporal resolution would enable matching the water samples from the specific days to the FUI, hence defining a more accurate relationship between the FUI and in situ data. Furthermore, this paper identifies CDOM as an additional parameter to be analysed alongside SPM, turbidity, salinity and nutrients in the future, to provide a more complete assessment of the relationship between the FUI and the water quality parameters. Overall, this paper presents a new water quality assessment typology, based on the ocean colour satellite product and FUI, which could be implemented into the UK water monitoring programs as an objective, repetitive, cost-effective and fast method of estimating water quality condition and the impact of land-based loads into the coastal marine environment.

Supplementary Materials: The following supporting information can be downloaded at: <https://www.mdpi.com/article/10.3390/rs14102375/s1>, Table S1. Description of the input data layers (* denotes data were acquired through a data request to the relevant organization). Figure S1. Spatial changes observed in the river plume extent ($FUI > 10$) in 2018 suggest the presence of three seasons: 1. wet season (months: 12, 1, 2, 3); 2. dry season (months: 5, 6, 7, 8) and 3. mixed season (months: 4, 9, 10, 11). Figure S2. Spatial changes observed in the river plume extent ($FUI \geq 10$) in 2020 suggest the presence of three seasons: 1. wet season (months: 12, 1, 2, 3); 2. dry season (months: 5, 6, 7, 8) and 3. mixed season (months: 4, 9, 10, 11). Figure S3. Spatial changes observed in the river plume extent ($FUI \geq 10$) in 2017 do not show the presence of the three seasons: wet, dry and mixed. The river plume across all months in 2017 is relatively constant. Figure S4. Kernel density distribution of the river plume data between 2017–2020. Figure S5. Q-Q plots showing a non-normal distribution of river plume and river flow data. Figure S6. Q-Q plots for all the in situ collected data and FUI show a non-normal distribution.

Author Contributions: Conceptualization, M.J.D., N.G., R.M. and L.F.; methodology, L.F., R.M., N.G., M.J.D., J.A.G., C.A.G. and C.P.; formal analysis, L.F., R.M., J.A.G., N.G., C.A.G. and R.H.; writing—original draft preparation, M.J.D.; writing—review and editing, L.F., N.G., M.J.D., C.P. and J.A.G.; funding acquisition, M.J.D. and N.G. All authors have read and agreed to the published version of the manuscript.

Funding: This research was funded by Department for Environment, Food and Rural Affairs (DEFRA), grant number GiA03, and Cefas through various projects (DP423 and DP434—internal Cefas projects, C8395—GIA OSPAR support, C8374—Ocean Country Partnership Programme).

Data Availability Statement: Publicly available datasets were analysed in this study. This data can be found here: Sentinel-3 A and B—<https://codarep.eumetsat.int>; <https://coda.eumetsat.int>, accessed on 20 December 2020; Authentication—EUMETSAT—EO Portal User Registration, River Flow data—<http://nrfa.ceh.ac.uk/data/search>, accessed on 20 December 2020, Water samples—The water sample data are available under the Open Government Licence (OGL) that can be found at <http://www.nationalarchives.gov.uk/doc/open-government-licence/version/3/>, accessed on 20 April 2020. The data can be accessed directly or on a request (*) from the following: Environment Agency (EA)—Open WIMS data, Natural Resources Wales *—“Contains Natural Resources Wales information © Natural Resources Wales and database right. All rights reserved.” <https://naturalresources.wales/evidence-and-data/accessing-our-data/request-environmental-data/?lang=en>, accessed on 20 May 2020, The Centre for Environment Fisheries and Aquaculture Science (Cefas)*—<https://data.cefas.co.uk/>, accessed on 20 April 2020, Agri-Food and Biosciences Institute (Afbi)*—<https://www.afbini.gov.uk/>, accessed on 20 April 2020.

Acknowledgments: We would like to thank the many staff members from Afbi, NRW, Cefas and the EA for provision of water quality data, including the sample collection, analysis and data curation. We would like to kindly thank Tiago Silva for reviewing and curating the final manuscript and for the expertise he provided in relation to remote sensing.

Conflicts of Interest: The authors declare no conflict of interest.

References

1. UK National Report. River Basin Management Plans: 2015. 2016. Available online: <https://www.gov.uk/government/collections/river-basin-management-plans-2015> (accessed on 18 October 2021).
2. Greenwood, N.; Devlin, M.J.; Best, M.; Fronkova, L.; Graves, C.A.; Milligan, A.; Barry, J.; Van Leeuwen, S.M. Utilizing Eutrophication Assessment Directives from Transitional to Marine Systems in the Thames Estuary and Liverpool Bay, UK. *Front. Mar. Sci.* **2019**, *6*, 116. [CrossRef]
3. Foden, J.; Sivy, D.B.; Mills, D.K.; Devlin, M.J. Spatial and Temporal Distribution of Chromophoric Dissolved Organic Matter (CDOM) Fluorescence and Its Contribution to Light Attenuation in UK Waterbodies. *Estuar. Coast. Shelf Sci.* **2008**, *79*, 707–717. [CrossRef]
4. UK National Report. Common Procedure for the Identification of the Eutrophication Status of the UK Maritime Area. 2017. Available online: http://randd.defra.gov.uk/Document.aspx?Document=ME2205_7330_FRP.pdf (accessed on 18 October 2021).
5. Garaba, S.P.; Friedrichs, A.; Voß, D.; Zielinski, O. Classifying Natural Waters with the Forel-Ule Colour Index System: Results, Applications, Correlations and Crowdsourcing. *Int. J. Environ. Res. Public Health* **2015**, *12*, 16096–16109. [CrossRef] [PubMed]
6. Van der Woerd, H.J.; Wernand, M.; Peters, M.; Bala, M.; Brochmann, C. True Color Analysis of Natural Waters with SeaWiFS, MODIS, MERIS and OLCI by SNAP. In Proceedings of the Ocean Optics XXIII, Victoria, BC, Canada, 23–28 October 2016.
7. Van der Woerd, H.J.; Wernand, M.R. Hue-Angle Product for Low to Medium Spatial Resolution Optical Satellite Sensors. *Remote Sens.* **2018**, *10*, 180. [CrossRef]
8. Petus, C.; Collier, C.; Devlin, M.; Rasheed, M.; McKenna, S. Using MODIS Data for Understanding Changes in Seagrass Meadow Health: A Case Study in the Great Barrier Reef (Australia). *Mar. Environ. Res.* **2014**, *98*, 68–85. [CrossRef]
9. Petus, C.; Devlin, M.; da Silva, E.T.; Lewis, S.; Waterhouse, J.; Wenger, A.; Bainbridge, Z.; Tracey, D. Defining Wet Season Water Quality Target Concentrations for Ecosystem Conservation Using Empirical Light Attenuation Models: A Case Study in the Great Barrier Reef (Australia). *J. Environ. Manag.* **2018**, *213*, 451–466. [CrossRef]
10. Petus, C.; da Silva, E.T.; Devlin, M.; Wenger, A.S.; Álvarez-Romero, J.G. Using MODIS Data for Mapping of Water Types within River Plumes in the Great Barrier Reef, Australia: Towards the Production of River Plume Risk Maps for Reef and Seagrass Ecosystems. *J. Environ. Manag.* **2014**, *137*, 163–177. [CrossRef]
11. Petus, C.; Waterhouse, J.; Lewis, S.; Vacher, M.; Tracey, D.; Devlin, M. A Flood of Information: Using Sentinel-3 Water Colour Products to Assure Continuity in the Monitoring of Water Quality Trends in the Great Barrier Reef (Australia). *J. Environ. Manag.* **2019**, *248*, 109255. [CrossRef]
12. Devlin, M.J.; Petus, C.; Da Silva, E.; Tracey, D.; Wolff, N.H.; Waterhouse, J.; Brodie, J. Water Quality and River Plume Monitoring in the Great Barrier Reef: An Overview of Methods Based on Ocean Colour Satellite Data. *Remote Sens.* **2015**, *7*, 12909–12941. [CrossRef]
13. Petus, C.; Devlin, M.; Thompson, A.; McKenzie, L.; Teixeira da Silva, E.; Collier, C.; Tracey, D.; Martin, K. Estimating the Exposure of Coral Reefs and Seagrass Meadows to Land-Sourced Contaminants in River Flood Plumes of the Great Barrier Reef: Validating a Simple Satellite Risk Framework with Environmental Data. *Remote Sens.* **2016**, *8*, 210. [CrossRef]
14. Waterhouse, J.; Gruber, R.; Logan, M.; Petus, C.; Howley, C.; Lewis, S.; Tracey, D.; James, C.; Mellors, J.; Tonin, H.; et al. *Marine Monitoring Program: Annual Report for Inshore Water Quality Monitoring 2019–20*; Great Barrier Reef Marine Park Authority: Townsville, Australia, 2021.
15. Forel, F. *Couleur de L'Eau in Optique, Le Léman. Monographie Limnologique*, 2nd ed.; Slatkine: Genève, Switzerland, 1895.

16. Ule, W. *Die Bestimmung der Wasserfarbe in Den Seen. Kleinere Mittheilungen. Dr. A. Petermanns Mittheilungen Aus Justus Perthes Geographischer Anstalt*; Justus Perthes: Gotha, Germany, 1892; pp. 70–71.
17. Cie, C. *Commission International de l'Eclairage Proceedings 1931*; Cambridge University: Cambridge, UK, 1932.
18. Novoa, S.; Wernand, M.; Van der Woerd, H. The Forel-Ule Scale Revisited Spectrally: Preparation Protocol, Transmission Measurements and Chromaticity. *J. Eur. Opt. Soc. Rapid Publ.* **2013**, *8*, 13057. [[CrossRef](#)]
19. Woerd, H.J.; Wernand, M.R. True Colour Classification of Natural Waters with Medium-Spectral Resolution Satellites: SeaWiFS, MODIS, MERIS and OLCI. *Sensors* **2015**, *15*, 25663–25680. [[CrossRef](#)] [[PubMed](#)]
20. Pitarch, J.; van der Woerd, H.J.; Brewin, R.J.; Zielinski, O. Optical Properties of Forel-Ule Water Types Deduced from 15 Years of Global Satellite Ocean Color Observations. *Remote Sens. Environ.* **2019**, *231*, 111249. [[CrossRef](#)]
21. Busch, J.A.; Price, I.; Jeansou, E.; Zielinski, O.; van der Woerd, H.J. Citizens and Satellites: Assessment of Phytoplankton Dynamics in a NW Mediterranean Aquaculture Zone. *Int. J. Appl. Earth Obs. Geoinf.* **2016**, *47*, 40–49. [[CrossRef](#)]
22. Wernand, M.; Hommersom, A.; van der Woerd, H.J. MERIS-Based Ocean Colour Classification with the Discrete Forel-Ule Scale. *Ocean Sci.* **2013**, *9*, 477–487. [[CrossRef](#)]
23. EyeOnWater. NIOZ, Veerder, MARIS and Citclops Project Partners. Available online: <https://www.eyeonwater.org/apps/eyeonwater-colour> (accessed on 24 January 2022).
24. Novoa, S.; Wernand, M.; van der Woerd, H.J. WACODI: A Generic Algorithm to Derive the Intrinsic Color of Natural Waters from Digital Images. *Limnol. Oceanogr. Methods* **2015**, *13*, 697–711. [[CrossRef](#)]
25. Garaba, S.P.; Voß, D.; Zielinski, O. Physical, Bio-Optical State and Correlations in North-Western European Shelf Seas. *Remote Sens.* **2014**, *6*, 5042–5066. [[CrossRef](#)]
26. Wooldridge, S.A. Water Quality and Coral Bleaching Thresholds: Formalising the Linkage for the Inshore Reefs of the Great Barrier Reef, Australia. *Mar. Pollut. Bull.* **2009**, *58*, 745–751. [[CrossRef](#)]
27. Wooldridge, S.A.; Done, T.J. Improved Water Quality Can Ameliorate Effects of Climate Change on Corals. *Ecol. Appl.* **2009**, *19*, 1492–1499. [[CrossRef](#)]
28. McKenzie, L.; Collier, C.; Waycott, M.; Unsworth, R.; Yoshida, R.; Smith, N. Monitoring Inshore Seagrasses of the GBR and Responses to Water Quality. In Proceedings of the 12th International Coral Reef Symposium, Cairns, Australia, 9–13 July 2012.
29. Collier, C.; Waycott, M.; McKenzie, L. Light Thresholds Derived from Seagrass Loss in the Coastal Zone of the Northern Great Barrier Reef, Australia. *Ecol. Indic.* **2012**, *23*, 211–219. [[CrossRef](#)]
30. Unsworth, R.K.; Collier, C.J.; Waycott, M.; Mckenzie, L.J.; Cullen-Unsworth, L.C. A Framework for the Resilience of Seagrass Ecosystems. *Mar. Pollut. Bull.* **2015**, *100*, 34–46. [[CrossRef](#)] [[PubMed](#)]
31. Polton, J.A.; Palmer, M.R.; Howarth, M.J. Physical and Dynamical Oceanography of Liverpool Bay. *Ocean Dyn.* **2011**, *61*, 1421. [[CrossRef](#)]
32. Krausova, A.; Vargas-Silva, C. North East: Census Profile 2013. Available online: http://migrationobservatory.ox.ac.uk/wp-content/uploads/2016/04/CensusProfile-North_East.pdf (accessed on 18 December 2021).
33. Turner, G. *Summary Statistics for North Wales Region: 2020*; Welsh Government: Welsh, UK, 2020.
34. Department for Environment, Food and Rural Affairs. *Defra Statistics: Agricultural Facts England Regional Profiles*; Department for Environment, Food and Rural Affairs: London, UK, 2021.
35. Greenwood, N.; Hydes, D.J.; Mahaffey, C.; Wither, A.; Barry, J.; Sivyver, D.B.; Pearce, D.J.; Hartman, S.E.; Andres, O.; Lees, H.E. Spatial and Temporal Variability in Nutrient Concentrations in Liverpool Bay, a Temperate Latitude Region of Freshwater Influence. *Ocean Dyn.* **2011**, *61*, 2181–2199. [[CrossRef](#)]
36. Devlin, M.J.; Barry, J.; Mills, D.K.; Gowen, R.J.; Foden, J.; Sivyver, D.; Greenwood, N.; Pearce, D.; Tett, P. Estimating the Diffuse Attenuation Coefficient from Optically Active Constituents in UK Marine Waters. *Estuar. Coast. Shelf Sci.* **2009**, *82*, 73–83. [[CrossRef](#)]
37. JNCC. Liverpool Bay/Bae Lerpwl SPA. 2020. Available online: <https://jncc.gov.uk/our-work/liverpool-bay-spa/> (accessed on 5 February 2022).
38. Moore, A.B.; Bater, R.; Lincoln, H.; Robins, P.; Simpson, S.J.; Brewin, J.; Cann, R.; Chapman, T.; Delargy, A.; Heney, C.; et al. Bass and Ray Ecology in Liverpool Bay. 2020. Available online: https://www.nw-ifca.gov.uk/app/uploads/Agenda-Item-12-Annex-A-Bass_ray_ecology_Liverpool_Bay_3.1_Final.pdf (accessed on 10 February 2022).
39. Marine Management Organisation (MMO). *Biodiversity, Habitats, Flora and Fauna-Protected Sites and Species*; MMO: Newcastle, UK, 2016.
40. European Space (ESA). *Sentinel-3 OLCI User Guide*; European Space Agency (ESA): Paris, France, 2018. Available online: <https://earth.esa.int/eogateway/documents/20142/1564943/Sentinel-3-OLCI-Marine-User-Handbook.pdf> (accessed on 15 January 2022).
41. Wyznecki, G.; Stiles, W.S. *Colour Science: Concepts and Methods, Quantitative Data and Formulae*; John Wiley & Sons: New York, NY, USA, 1982.
42. Pitarch, J.; Bellacicco, M.; Marullo, S.; Van Der Woerd, H.J. Global Maps of Forel-Ule Index, Hue Angle and Secchi Disk Depth Derived from 21 Years of Monthly ESA Ocean Colour Climate Change Initiative Data. *Earth Syst. Sci. Data* **2021**, *13*, 481–490. [[CrossRef](#)]
43. Seneviratne, S.; Nicholls, N.; Easterling, D.; Goodess, C.; Kanae, S.; Kossin, J.; Luo, Y.; Marengo, J.; McInnes, K.; Rahimi, M.; et al. Changes in Climate Extremes and Their Impacts on the Natural Physical Environment. *Acad. Commons* **2012**, 109–230. [[CrossRef](#)]
44. Thewes, D.; Stanev, E.; Zielinski, O. The North Sea Light Climate: Analysis of Observations and Numerical Simulations. *J. Geophys. Res. Ocean.* **2021**, *126*, e2021JC017697. [[CrossRef](#)]

45. Wollschläger, J.; Neale, P.J.; North, R.L.; Striebel, M.; Zielinski, O. Climate Change and Light in Aquatic Ecosystems: Variability & Ecological Consequences. *Front. Mar. Sci.* **2021**, *8*, 506.
46. Opdal, A.F.; Lindemann, C.; Aksnes, D.L. Centennial Decline in North Sea Water Clarity Causes Strong Delay in Phytoplankton Bloom Timing. *Glob. Chang. Biol.* **2019**, *25*, 3946–3953. [[CrossRef](#)]
47. Brodie, J.; Waterhouse, J.; Maynard, J.; Bennett, J.; Furnas, M.; Devlin, M.; Lewis, S.; Collier, C.; Schaffelke, B.; Fabricius, K.; et al. Assessment of the Relative Risk of Water Quality to Ecosystems of the Great Barrier Reef. A Report to the Department of the Environment and Heritage Protection, Queensland Government, Brisbane-Report 13/28. 2013. Available online: https://www.researchgate.net/publication/285590901_Assessment_of_the_relative_risk_of_water_quality_to_ecosystems_of_the_Great_Barrier_Reef_A_report_to_the_Department_of_the_Environment_and_Heritage_Protection_Queensland_Government_Brisbane_-_Report_1 (accessed on 10 January 2022).